


## RESEARCH ARTICLE

# The anti-HIV drug nelfinavir mesylate (Viracept) is a potent inhibitor of cell fusion caused by the SARSCoV-2 spike (S) glycoprotein warranting further evaluation as an antiviral against COVID-19 infections

Farhana Musarrat PhD<sup>1,2</sup> | Vladimir Chouljenko PhD<sup>1,2</sup> | Achyut Dahal<sup>3</sup> |  
Rafiq Nabi PhD<sup>1,2</sup> | Tamara Chouljenko MS<sup>4</sup> | Seetharama D. Jois PhD<sup>3</sup> |  
Konstantin G. Kousoulas PhD<sup>1,2</sup> 

<sup>1</sup>Division of Biotechnology and Molecular Medicine, Louisiana State University, Baton Rouge, Louisiana

<sup>2</sup>Department of Pathobiological Sciences, School of Veterinary Medicine, Louisiana State University, Baton Rouge, Louisiana

<sup>3</sup>School of Basic Pharmaceutical and Toxicological Sciences, College of Pharmacy, University of Louisiana Monroe, Monroe, Louisiana

<sup>4</sup>Louisiana State University Agricultural Center, Agricultural Biotechnology Laboratory, Baton Rouge, Louisiana

## Correspondence

Konstantin G. Kousoulas, PhD, Division of Biotechnology and Molecular Medicine, Louisiana State University, Baton Rouge, LA 70803.

Email: [vtgusk@su.edu](mailto:vtgusk@su.edu)

## Funding information

Louisiana Board of Regents Governor's Biotechnology Initiative, Grant/Award Number: KGK; The School of Veterinary Medicine, Division of Biotechnology & Molecular Medicine (BioMMED) and Core Facilities, Grant/Award Numbers: NIGMS P20 GM103424 (Louisiana Biomedical Research Network), NIGMS P20GM130555 (Center for Lung Biology).

## Abstract

Severe acute respiratory syndrome coronavirus-2 (SARS CoV-2) is the causative agent of the coronavirus disease-2019 (COVID-19) pandemic. Coronaviruses enter cells via fusion of the viral envelope with the plasma membrane and/or via fusion of the viral envelope with endosomal membranes after virion endocytosis. The spike (S) glycoprotein is a major determinant of virus infectivity. Herein, we show that the transient expression of the SARS CoV-2 S glycoprotein in Vero cells caused extensive cell fusion (formation of syncytia) in comparison to limited cell fusion caused by the SARS S glycoprotein. Both S glycoproteins were detected intracellularly and on transfected Vero cell surfaces. These results are in agreement with published pathology observations of extensive syncytia formation in lung tissues of patients with COVID-19. These results suggest that SARS CoV-2 is able to spread from cell-to-cell much more efficiently than SARS effectively avoiding extracellular neutralizing antibodies. A systematic screening of several drugs including cardiac glycosides and kinase inhibitors and inhibitors of human immunodeficiency virus (HIV) entry revealed that only the FDA-approved HIV protease inhibitor, nelfinavir mesylate (Viracept) drastically inhibited S-n- and S-o-mediated cell fusion with complete inhibition at a 10- $\mu$ M concentration. In-silico docking experiments suggested the possibility that nelfinavir may bind inside the S trimer structure, proximal to the S2 amino terminus directly inhibiting S-n- and S-o-mediated membrane fusion. Also, it is possible that nelfinavir may act to inhibit S proteolytic processing within cells. These results warrant further investigations of the potential of nelfinavir mesylate to inhibit virus spread at early times after SARS CoV-2 symptoms appear.

## KEYWORDS

antiviral agents, cell fusion, cellular effect, coronavirus, entry inhibitors, fusion protein, glycoproteins, infection, SARS coronavirus, virus classification

## 1 | INTRODUCTION

The severe acute respiratory syndrome coronavirus-2 (SARS CoV-2) is currently associated with a global pandemic causing coronavirus disease, first noted in December 2019 in Wuhan province of China. The resultant disease is termed COVID-19 (coronavirus disease-2019) and is characterized by acute respiratory disease and pneumonia. SARS CoV-2 has infected nearly 4 million people and caused nearly 300 000 deaths worldwide with a predilection of older people and/or people having other health issues including, hypertension, diabetes, obesity, and other comorbidities.<sup>1-3</sup> SARS-CoV-2 is the third human coronavirus that appeared for the first time in the 21st century. One of the other two coronaviruses is SARS, which appeared in November 2002 in China and caused nearly 100 000 infections worldwide and more than 800 deaths. SARS was effectively contained because the virus, although causing high degree of mortality in infected people, was apparently not effectively transmitted from one person to the other.<sup>4,5</sup> The second human coronavirus, Middle East Respiratory Syndrome Coronavirus (MERS CoV) appeared in 2013 and caused a limited epidemic of few thousand people, but high death rates of approximately 36% predominantly in the Middle East (Saudi Arabia). The primary source of infection was found to be dromedary camels, although the virus was transmitted from person to person in close contact in hospital settings.<sup>6-9</sup>

All coronaviruses specify a spike (S) glycoprotein, which is embedded in viral envelopes in trimeric forms giving them their characteristic corona structures. The S glycoprotein is a major antigen responsible for both receptor-binding and membrane fusion properties.<sup>9</sup> Angiotensin-converting enzyme 2 (ACE2) has been identified as the cell receptor for SARS,<sup>10</sup> and also SARS CoV-2, while other unknown human receptors may be responsible for its wider infectious spread than SARS. Spike is cleaved into two major components S1 and S2 by cellular proteases. Virus entry into cells is mediated after binding of a receptor-binding domain (RBD) located within the S1 ectodomain. Cleavage of the S glycoprotein to produce S1 and S2 proteins is mediated by cellular proteases at the S1/S2 junction as well as at S2' site located downstream of the S1/S2 proteolytic cleavage. The fusion of the viral envelope with cellular membranes is mediated by the S2 protein that contains a putative fusion peptide region. The mechanism of membrane pore formation that leads to membrane fusion involves the formation of a six-helix bundle fusion core by two heptad repeats HR1 and HR2 domains found in each S monomer forming the initial pore that results in membrane fusion.<sup>11</sup> The cellular serine protease TMPRSS2 has been implicated in priming S2' cleavage, as well as ACE2 cleavage both required for initiation of the membrane fusion event.<sup>12-14</sup> Also, the SARS Spike (S) glycoprotein can be cleaved by the cellular protease cathepsin L at the low pH of endosomes, thereby exposing the S2 domain of the spike protein for membrane fusion.<sup>15-20</sup> Cell surface expression of S mediates S-induced cell fusion and the formation of syncytia, which is a phenomenon similar to virus entry, requiring the presence of ACE2. Virus-induced cell fusion is a mechanism by which the virus can spread from cell-to-cell by a pH-independent mechanism avoiding the extracellular space and potentially evading neutralizing antibody.<sup>21,22</sup> It has

been demonstrated that the RBD domain of SARS CoV-2 Spike (S-new; Sn) has a higher binding affinity for the ACE2 receptor than that of SARS Spike (S-old; So), while the S2 proteins of these two viruses are nearly 90% identical.<sup>3,22,23</sup>

Nelfinavir mesylate was developed as an anti-human immunodeficiency virus (HIV) protease inhibitor.<sup>24,25</sup> Also, it was reported that nelfinavir mesylate inhibited SARS replication and cytopathic effects in cell culture.<sup>26</sup> In addition to its potent activity against the HIV protease, nelfinavir mesylate was found to produce multiple effects on cellular processes including the induction of apoptosis and necrosis as well as induction of cell-protective mechanisms, including cell cycle retardation and the unfolded protein response.<sup>27-29</sup> These nelfinavir mesylate effects have been exploited for anticancer purposes.<sup>30-32</sup>

Previously, we investigated the structure and function of the SARS S glycoprotein in transient transfection-membrane fusion assays.<sup>33,34</sup> Based on these initial studies, we undertook screening of a number of compounds that may inhibit S-mediated fusion after transient expression in African green monkey kidney cells (Vero). We report herein that the SARS CoV-2 S (Sn) causes extreme S-mediated membrane fusion in comparison to cell fusion caused by transient expression of SARS S (So). Importantly, we report that nelfinavir mesylate inhibited S-mediated fusion at micromolar ranges. In-silico docking experiments, revealed the possibility that nelfinavir binds to the S2 amino terminus within the S trimer and thus, may directly inhibit the formation of the heptad-repeat complex that causes S-mediated membrane fusion. Based on these results, further research of nelfinavir's effect in human COVID-19 patients is warranted.

## 2 | MATERIALS AND METHODS

### 2.1 | Cell line

African green monkey kidney (Vero) cells were maintained in Dulbecco's modified Eagle's medium (DMEM) with 10% fetal bovine serum (FBS) and 2% primocin (Invitrogen, Inc., Carlsbad, CA).

### 2.2 | Reagents and antibodies

Nelfinavir mesylate was bought from R&D Systems, Inc (MN) and dimethyl sulfoxide (DMSO) was bought from Sigma, Inc (St Louis, MO). The primary antibodies used were as follows: mouse anti-MYC antibody (Abcam), mouse anti-FLAG antibody (Abcam). Goat anti-mouse antibody conjugated with horseradish peroxidase (HRP) was used as a secondary antibody. The Vector Nova Red peroxidase (HRP) substrate kit (Vector Laboratories, Burlingame, CA) was used for imaging. Goat anti-mouse antibody conjugated with Alexa fluorophore 647 and goat anti-rabbit antibody conjugated with Alexa fluorophore 488 (Invitrogen, Inc.) were used for immunofluorescence assay. IRDye goat anti-mouse and goat anti-rabbit antibody (LI-COR Biotechnology, Lincoln, NE) were used for immunoprecipitation assay.

## 2.3 | Construction of recombinant spike proteins

The SARS and SARS CoV-2 Spike expression plasmids used in the present study were constructed in a very similar manner. Both S genes were placed under the control of the human cytomegalovirus (CMV) immediate early promoter and were engineered to contain either 3XFLAG or N-MYC epitope tags at their amino terminal ends, respectively. These S-n and S-o genes were cloned into p3XFLAG-CMV-9 (Sigma, MO) and pCMV3-SP-N-MYC (Sino Biological, PA) parental vector plasmids, respectively. The S1 subunit of the S-n expression construct contained the same amino terminus up to aa700 (Gly). The N-terminal domain of the S-n S2 subunit was engineered to be exactly as in S1 containing the N-MYC tag at its amino terminus and encompassing the S2 S-n amino acid sequence 701-1273.

## 2.4 | Transient transfection assay

Vero cells were grown on 24-well plates and transiently transfected with either pCMV3-SP-N-MYC (Sn) or p3XFLAG-CMV-S (So) using lipofectamine 2000 reagent. Approximately, 2  $\mu$ L of lipofectamine and 0.5  $\mu$ g of plasmid DNA was used for transfection of Vero cells. Appropriate controls were also used. Following 48 hours, the plates were examined by phase contrast microscopy for fused cells and images were taken under live conditions, as well as either after formalin or methanol fixation. Cells were stained for FLAG (So, mouse anti-FLAG-1:2500) or N-MYC (Sn, mouse anti-MYC-1:500) with HRP (Vector Nova Red stain kit) for phase contrast microscopy. Similarly, cells were stained for fluorescent microscopy using anti-mouse antibody conjugated with Alexa fluorophore 647 (1:100) and anti-rabbit antibody conjugated with Alexa fluorophore 488 (1:100).

## 2.5 | Drug inhibition of cell fusion assay

Nelfinavir mesylate was dissolved in DMSO at a 10 mM concentration (stock) and a series of dilutions was made in serum-free DMEM. Following transfection, 500  $\mu$ L of nelfinavir mesylate solution was added to each well. Vero cells transfected with either S-o or S-n and incubated with the drug for 48 hours at 37°C with 5% CO<sub>2</sub>. The tissue culture plates were observed for fused cells, and then, phase contrast and fluorescent images were taken under either formalin or methanol fixed conditions.

## 2.6 | Computational methods

Docking of the nelfinavir mesylate to the spike protein of SARS CoV-2 was performed using Autodock.<sup>35</sup> Crystal structure of nelfinavir was obtained from the complex of HIV protease nelfinavir crystal structure from the protein data bank (PDB ID: 2Q64).<sup>36</sup> Structure of the S protein of SARS CoV-2 was reported by Wrapp

et al<sup>23</sup> (PDB ID: 6VSB). The trimer structure of the spike protein was used for docking as protein structure of the spike protein exists under dynamic condition while binding to the receptor and fusion to host cell. Grid for docking was created on the spike protein structure at particular docking site as the center but covering a grid box of 102 or 126 Å in X, Y, Z directions from the center of the grid. One grid site was created around protease cleavage site S1/S2 and another covering the HR1 region of the protein in the trimer (Figure S1). Docking calculations were performed using the Lamarckian genetic algorithm with 150 starting conformations and 10 million energy evaluations. Fifty low energy docked structures were used for final analysis. Structures within 2 kcal/mol from the lowest energy docked structures were represented as final possible docked structures using PyMol software (Schrodinger). The lowest energy docked structure was bound near the helices of HR1 region with a docking energy of -10.57 kcal/mol. Although the docking grid was created to cover the S1/S2 cleavage site, the low energy docked structure of nelfinavir was bound in the pocket between the helices of fusion peptide and HR1 region and lower part of NTD region (Figure S2). The docking energy of the nelfinavir bound structure was -9.98 kcal/mol. In the lowest energy docked conformation, the nelfinavir- SARS CoV-2 spike complex was stabilized by three hydrogen bonds and hydrophobic interactions. T768 from S protein fusion peptide formed two hydrogen bonds and Q957 of HR1 helix formed one hydrogen bond with nelfinavir. Hydrophobic interaction was dominated by aromatic functional groups of nelfinavir with Tyr313, Leu303, and Q314 side chains alkyl group in the S protein (Figure S2).

## 2.7 | Instruments and software

Olympus IX71 fluorescent microscope was used for live and phase contrast images using CellSens software. Zeiss Axio Observer Z1 fluorescent microscope was used for fluorescent images using Zen software.

# 3 | RESULTS

## 3.1 | SARS CoV-2 Spike (Sn) is significantly more fusogenic than SARS Spike (So)

Virus entry is facilitated by S-mediated fusion between the viral envelope and either cellular plasma membranes or endosomal membranes. S-mediated cell fusion is caused by cell surface expression of S and it is thought to be a surrogate model of both virus entry and cell fusion. Previously, we reported a detailed analysis of the functional domains of the SARS Spike (S) glycoprotein that are important for S-mediated membrane fusion and the formation of multinucleated cells (syncytia) including delineation of domains important for synthesis, cell surface expression, and endocytosis from cell surfaces (14, 15). To compare the S-o- vs S-n-mediated cell fusion, both genes were cloned into the traexpression vectors as codon-optimized genes

carrying a 3XFLAG or N-MYC epitope tags at their amino termini (Figure 1A,B,E,F). In addition, the S1 and S2 domains of S-n were cloned independently into the transient expression vector pCMV3, encompassing amino acid domains for S1 (aa16-aa700) and S2 (aa701-aa1273). Both S1 and S2 domains were expressed with an MYC epitope tag at their amino termini (Figure 1C,D). The S1 domain included the S1/S2 cleavage site (Figure 1C). Vero cells were transfected with the S-n- or S-o-expressing plasmids and were detected at 48 hours posttransfection (hpt) using anti-MYC and anti-FLAG antibodies in conjunction with secondary antibody linked to horseradish peroxidase (see Section 2). Vero cells were also transfected with plasmid vehicle controls or mock-transfected. Expression of both S-n and S-o was readily detected by immunohistochemistry, while there was no signal obtained from the Vero mock-transfected and HRP-stained control cell

monolayers. Phase contrast microscopy revealed the presence of extensive syncytia formation in S-n, but not S-o-transfected cells, while the remaining monolayer of cells did not exhibit any cellular toxicity (Figure 2A). Further examination of transfected Vero cells by immunofluorescence staining for cellular tubulin (anti-alpha tubulin antibody), nuclei (DAPI), and anti-N-MYC and anti-FLAG antibodies followed by anti-mouse fluorescent antibody provided additional support that untransfected monolayers appeared normal, while S-n expression produced large syncytia in contrast to much smaller syncytia formed after S-o transient expression (Figure 2B). Co-expression of S1 and S2 was performed to test whether the Sn-mediated cell fusion could be reconstituted by coexpression of both domains. Expression of either S1, S2, or S1 + S2 domains of S-n was readily detected by immunohistochemistry with the anti-N-MYC antibody; however, there

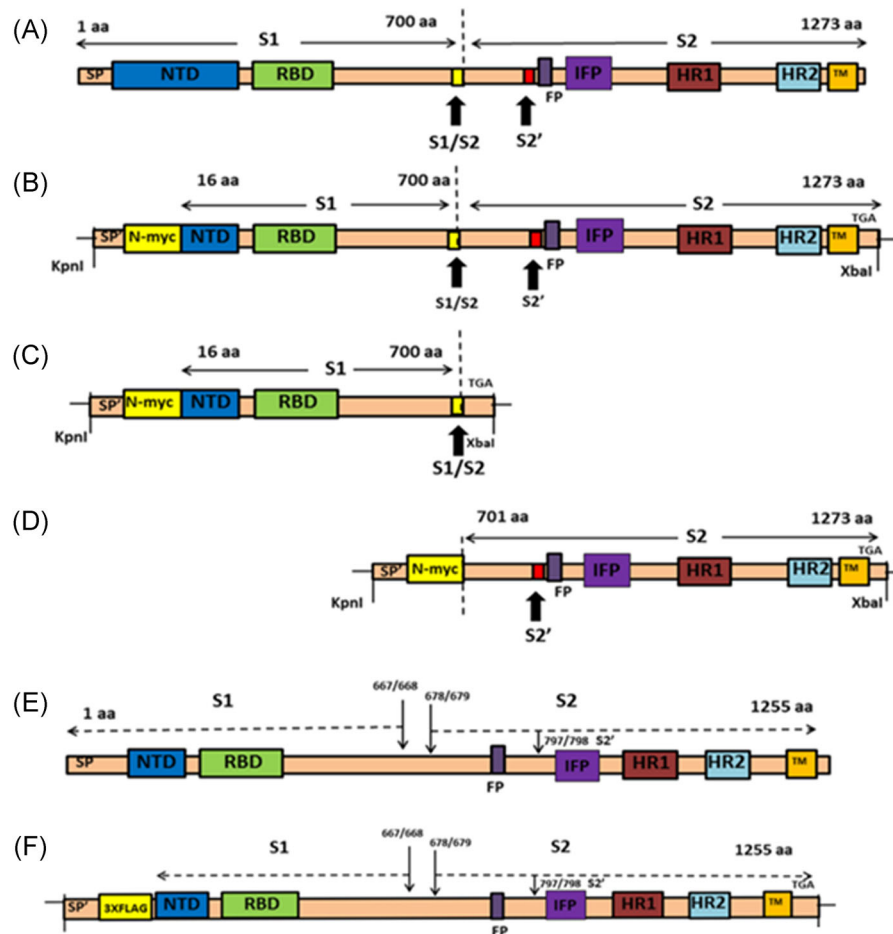


**FIGURE 1** Schematics of spike glycoproteins and recombinant gene constructs. (A) Structure of SARS-CoV-2 spike (1273aa) glycoprotein, showing S1 and S2 domains and the cleavage sites S1/S2 and S2'. (B) Structure of pCMV3-SP-N-MYC (Sn). SARS-CoV-2 spike (aa16-aa1273) was cloned into plasmid expression vector at KpnI and XbaI restriction sites. The N-terminal 15 amino acids were replaced with signal peptide (SP') and N-MYC sequence. (C) Structure of pCMV3-S1-N-MYC (S1-n). The S1 domain (aa16-aa700) was cloned into the plasmid expression vector at KpnI and XbaI restriction sites. The N-terminal 15 amino acids were replaced with signal peptide (SP') and N-MYC sequence. (D) Structure of pCMV3-S2-N-MYC (S2-n). The S2 domain (aa701-aa1273) was cloned at KpnI and XbaI restriction sites. The N-terminal contains signal peptide (SP') and N-MYC sequence. (E) Structure of SARS spike (1255aa) glycoprotein, showing S1 and S2 domains and the cleavage sites S1/S2 and S2'. (F) Structure of p3XFLAG-CMV-S (So). SARS spike was cloned into plasmid expression vector as previously described. FP, fusion peptide; HR1, heptad repeat 1; HR2, heptad repeat 2; NTD, nontranslated domain; RBD, receptor-binding domain; SARS CoV, severe acute respiratory syndrome coronavirus; SP, SARS signal peptide; SP', signal peptide

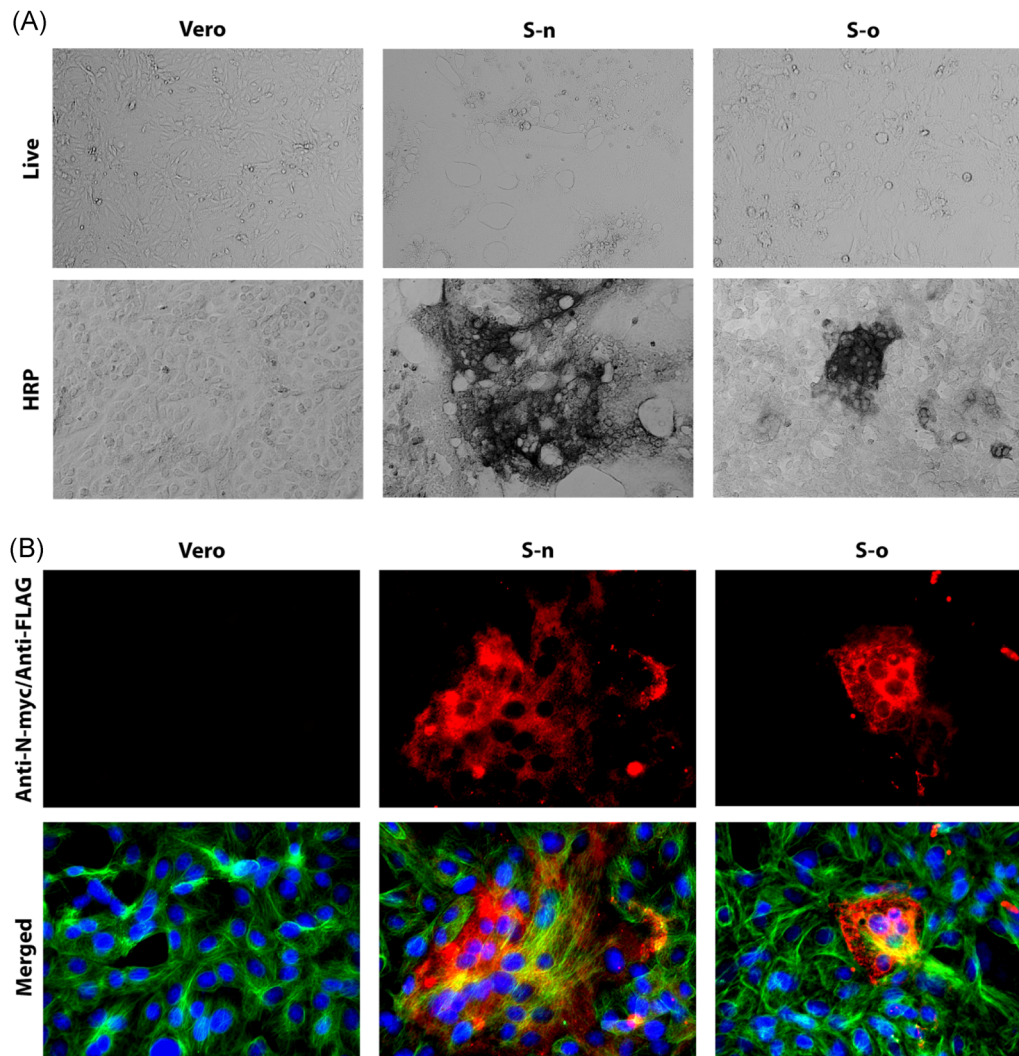


**FIGURE 2** Syncytia formation by S-n and S-o. Vero cells were transfected with plasmids expressing either the S-o or S-n glycoproteins tagged with the 3XFLAG and N-MYC epitopes at their amino termini, respectively. S-n and S-o expression was detected with mAbs against the epitope tags at 48 hours posttransfection and compared to vehicle containing equivalent amount of lipofectamine. Methanol fixed cells were incubated with mouse anti-N-MYC (Sn) (1:500 or 1:50) or mouse anti-FLAG (So) (1:2500 or 1:200) antibody and stained with either (A) HRP staining or (B) Alexa fluorophore 647 conjugated goat anti-mouse secondary antibody (1:1000). Cellular tubulin was stained with rabbit anti-alpha tubulin (1:200) and anti-rabbit secondary antibody conjugated with Alexa fluorophore 488 (1:1000). DAPI was used to stain nuclei of cells. Phase contrast images were taken at  $\times 10$  magnification, whereas the fluorescent images were taken at  $\times 40$  magnification. DAPI, 4',6-diamidino-2-phenylindole; HRP, horseradish peroxidase; S-n, S-new; S-o, S-old

was no cell fusion observed at 48 hpt as evidenced by only well-defined single cells that were stained with the anti-MYC antibody (Figure 3), as well as at later times (not shown), suggesting that the S1 and S2 domains have to be part of the entire molecule to be processed correctly for induction of S-mediated cell fusion.

### 3.2 | Nelfinavir drastically inhibits cell-to-cell fusion mediated by S-n and S-o without affecting cell surface expression

Transiently transfected Vero cells were treated with either DMSO, or a series of dilutions (100-0.001  $\mu\text{M}$ ) of nelfinavir

mesylate. Following 48 hpt, the cells were fixed with methanol and stained for either N-MYC (S-n) or FLAG (S-o) to detect S-n and S-o expression in transfected cells. Nelfinavir mesylate treatment did not inhibit overall S-n and S-o expression, as evidenced by the efficient expression and detection of both proteins via immunohistochemistry (Figure 4A,B). Both S-n and S-o mediated fusion was significantly inhibited by nelfinavir at a dose-dependent manner with complete inhibition observed at the lowest effective concentration of 10  $\mu\text{M}$  compared with the untreated control (Figure 4A,B). To determine the effect of nelfinavir on the surface expression of spike, we transiently transfected Vero cells with plasmids expressing either the S-o or S-n glycoproteins tagged with the 3XFLAG and N-MYC epitopes at

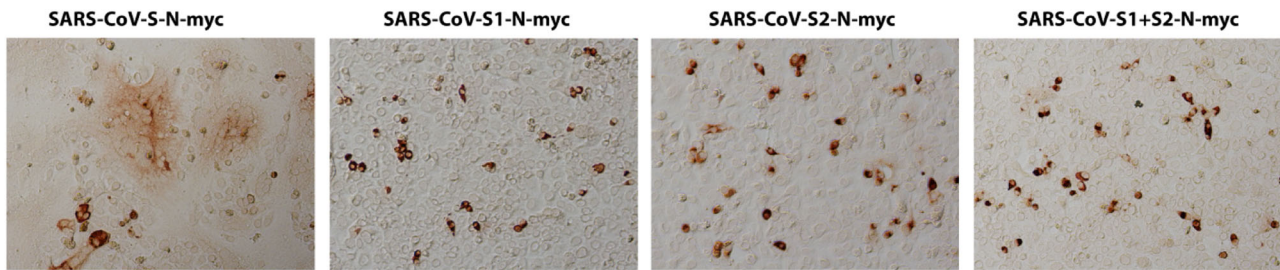


**FIGURE 3** Expression of SARS CoV-2 spike (Sn) domains. Vero cells were transfected with pCMV3-SP-N-MYC plasmid expressing either the S1, S2, or S1 + S2 domains of S-n tagged with the N-MYC epitopes at their amino termini. Expression was detected with mAbs against the epitope tags at 48 hours posttransfection and compared to vehicle containing equivalent amount of lipofectamine 2000 reagent. Methanol fixed cells were incubated with mouse anti-MYC antibody and stained with HRP staining followed by goat anti-mouse secondary antibody incubation. Images were taken at  $\times 10$  magnification. HRP, horseradish peroxidase; SARS CoV, severe acute respiratory syndrome coronavirus; Sn, S-new

their amino termini, respectively, and treated these cells with either nelfinavir ( $10 \mu\text{M}$ ) or DMSO control for 48 hours at  $37^\circ\text{C}$  with 5%  $\text{CO}_2$ . The cells were observed for characteristic syncytia formation and then fixed with either formalin or methanol to detect surface expression or endogenous expression of the spike glycoprotein following nelfinavir treatment, respectively. Although there were

significant differences in the number of fused cells (size of syncytia) following drug treatment, no apparent difference was visible in the surface expression of spike compared to total spike expression between S-n- and S-o-transfected cells. These experiments revealed that nelfinavir at concentrations that drastically inhibited cell fusion, did not affect S-n or S-o cell surface expression (Figure 5).

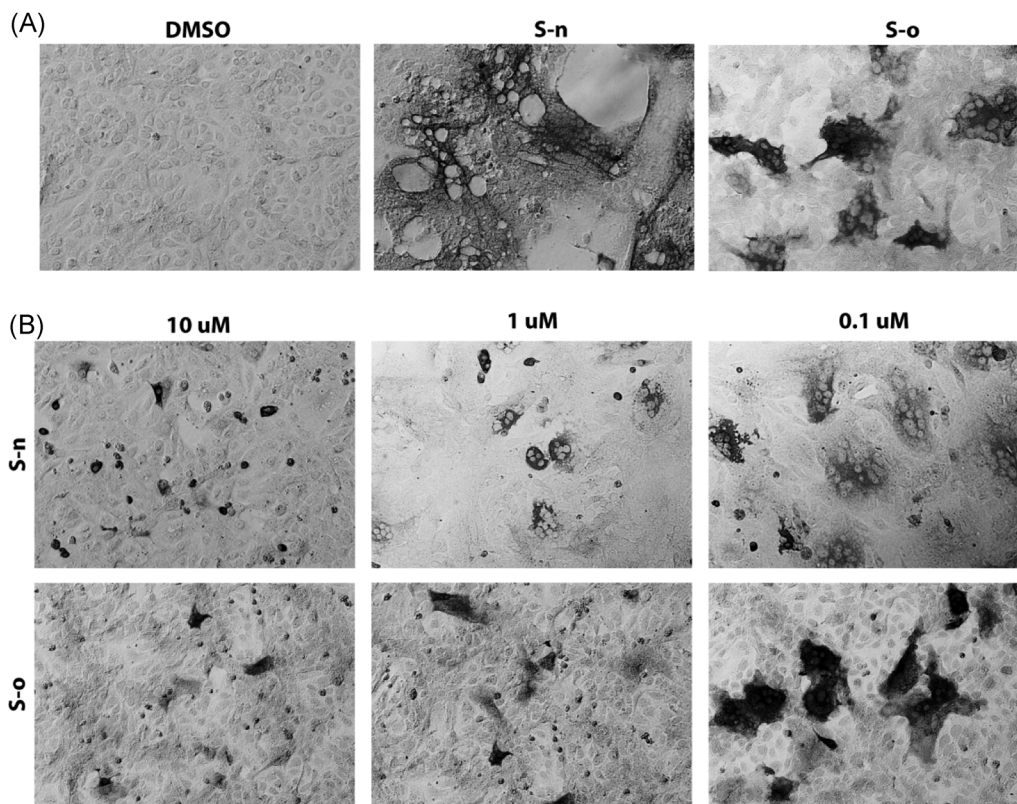


**FIGURE 4** Fusion inhibition by nelfinavir. (A) Vero cells were transfected with plasmids expressing either the S-o or S-n glycoproteins tagged with the 3XFLAG and N-MYC epitopes at their amino termini, respectively. S-n and S-o expression was detected with mAbs against the epitope tags at 48 hours posttransfection and compared to vehicle containing equivalent amount of DMSO. (B) S-n and S-o glycoproteins were expressed as in (A). Nelfinavir was added at the time of transfection at the concentrations indicated. Methanol fixed cells were incubated with mouse anti-MYC (S-n) or mouse anti-FLAG (S-o) antibody and stained with HRP staining followed by goat anti-mouse secondary antibody incubation. Images were taken at  $\times 10$  magnification. HRP, horseradish peroxidase; DMSO, dimethyl sulfoxide; Sn, S-new; So, S-old

### 3.3 | Computation modeling of nelfinavir–S-n potential interactions

Recently, it was shown that a peptide that targeted the S-n HR1 domain S inhibited SARS-CoV-2 virus replication, virus entry, and virus-induced cell fusion.<sup>37</sup> Therefore, we performed in-silico docking experiments to investigate the possibility that nelfinavir may directly bind near this S region. These theoretical docking experiments revealed that nelfinavir may bind near the HR1 helix and in between the HR1 and HR2 helices (Figures S1 and S2).

## 4 | DISCUSSION

Virus-induced cell fusion and the formation of multinucleated cells (syncytia) is the hallmark of many different viral infections including retroviruses, herpesviruses, coronaviruses, and other viruses. These membrane fusion phenomena are caused by expression of fusogenic glycoproteins on infected cell surfaces. Cell-to-cell fusion mediated by viral glycoproteins is similar to fusion of viral envelopes with cellular membranes that typically occur at the plasma membrane at physiological pH or after endocytosis of virion enveloped particles within endosomes followed by fusion of the viral envelope with endosomal membranes to release the nucleocapsid protein in the cytoplasm.<sup>38</sup> Virus-induced cell fusion is an important cytopathic phenomenon because the virus can spread from cell-to-cell avoiding extracellular spaces and exposure to neutralizing antibodies.<sup>39</sup> Virus-induced cell fusion can also cause hyperinflammatory responses

producing adverse effects in the infected host. Herein, we show that the SARS CoV-2 Spike (Sn) glycoprotein causes drastically more cell fusion and syncytia formation in comparison to the SARS Spike (So) glycoprotein following transient expression in Vero cells. Importantly, we show that nelfinavir mesylate, a currently prescribed anti-HIV protease inhibitor, drastically inhibited both S-n- and S-o-mediated cell fusion. These results indicate that it is highly likely that increased SARS CoV-2 virulence over SARS may be attributed to the enhanced fusogenicity exhibited by S-n in comparison to the S-o glycoprotein. Importantly, the fact the nelfinavir drastically inhibited S-n- and S-o-mediated cell fusion suggests that it should be used as an anti-SARS CoV-2 antiviral, especially at early times after first symptoms are exhibited in infected individuals.

Transient expression of S-n and S-o glycoproteins produced drastic differences in cell fusion, while their overall protein expression was similar, as evidenced by immunohistochemistry signals obtained at 48 hpt. The enhanced fusogenicity of SARS CoV-2 vs SARS CoV was recently noted in infection of Vero cells,<sup>37</sup> further validating that our transient transfection results reflect spike-mediated virus-induced cell fusion differences between SARS and SARS CoV-2. Cell surface expression of S-n and S-o was comparable suggesting that the observed differences in membrane fusion was due to inherent differences in the structure and function of S-n vs S-o glycoproteins. Interestingly, independent expression of S1 and S2 domains of S-n did not cause any cell fusion. It is not clear whether these two domains could be processed and expressed on cell surfaces, although the S-2 domain could be detected via immunohistochemistry (not shown). These results suggest that the entire S glycoprotein needs to be expressed in an

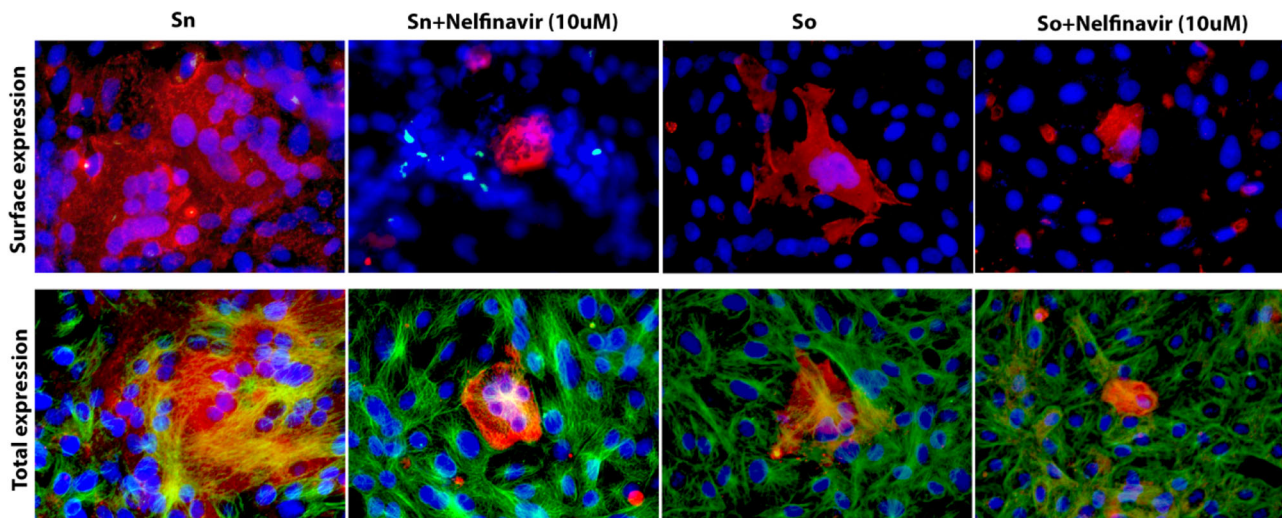


**FIGURE 5** Surface expression of spike glycoproteins. Vero cells were transfected with plasmids expressing either the S-o or S-n glycoproteins tagged with the 3XFLAG and N-MYC epitopes at their amino termini, respectively. S-n and S-o expression was detected with mAbs against the epitope tags at 48 hours posttransfection and compared to vehicle containing equivalent amount of DMSO. Nelfinavir was added at the time of transfection at the concentrations indicated. Formalin or Methanol fixed cells were incubated with mouse anti-N-MYC (Sn) (1:100) or mouse anti-FLAG (So) (1:200) antibody and stained with Alexa fluorophore 647 conjugated goat anti-mouse secondary antibody (1:1000). Cellular tubulin was stained with rabbit anti-alpha tubulin (Abcam; 1:200) and anti-rabbit secondary antibody conjugated with Alexa fluorophore 488. DAPI was used to stain nuclei of cells. Fluorescent images were taken at  $\times 40$  magnification. DAPI, 4',6-diamidino-2-phenylindole; DMSO, dimethyl sulfoxide; Sn, S-new; So, S-old

uncleaved form that may be proteolytically processed either within endosomes or at cell surfaces by proteases such as TMPRSS2, which is known to be required for Spike activation during virus entry.<sup>12</sup>

We utilized the S-n and S-o transient expression system to screen for currently available drugs that may inhibit S-mediated cell fusion and the formation of syncytia. These drugs included cardiac glycosides such as ouabain and digoxin, the anti-HIV fusion inhibitor Fuzeon (enfuvirtide) and kinase inhibitors including Gleevec (imatinib mesylate). These drugs did not substantially inhibit S-mediated cell fusion even at concentrations of 100  $\mu$ M. However, we found that nelfinavir mesylate, a known and currently prescribed anti-HIV drug drastically inhibited Sn- and So-mediated cell fusion at micromolar concentrations. The 10  $\mu$ M concentration used in our tissue culture experiments is approximately 10-fold lower than the observed AUC<sub>24</sub> (area under the plasma concentration-time curve during a 24-hour period) at steady state<sup>40</sup> (FDA Reference Document Viracept: ID:2910197). Therefore, it may be possible that nelfinavir can be used at even lower concentrations than those prescribed for patients with HIV. These results are significant because nelfinavir did not appear to inhibit overall S-n or S-o synthesis and cell surface expression. We considered the possibility that nelfinavir may act not as a protease inhibitor but as a direct inhibitor of spike-mediated membrane fusion. Computational modeling revealed that nelfinavir may directly bind to the trimeric form of S-n and S-o near the putative fusogenic domain, and thus, it may directly inhibit S-mediated cell fusion (Figures S1 and S2). Nelfinavir has been reported to have pleotropic effects on multiple cellular processes including inducing apoptosis an ER stress under certain conditions and has been investigated for anticancer purposes.<sup>32,41,42</sup> Thus, it is possible that cellular signaling processes are affected that alter to posttranslational processing of S-n and S-o, without affecting their cell surface expression. It is also possible that nelfinavir may inhibit cellular proteases including TMPRSS2 that may be required for S-n and S-o fusion activation. Other protease inhibitors are currently being investigated for their ability to inhibit SARS CoV-2 replication and spread. However, there are no concrete results that have been obtained in clinical trials yet.<sup>43</sup> Preliminary experiments indicate that S-n and S-o may be cleaved in Vero cells in the presence of nelfinavir, although it is not currently known whether this cleavage occurs efficiently. In addition, transfected cells expressing S-n or S-o in the presence of nelfinavir did not appear to exhibit morphologies indicating of cellular cytotoxicity, suggesting that nelfinavir is not cytotoxic at the concentrations used in this study. Overall, these experiments suggest that nelfinavir should be used to combat SARS CoV-2 infections early during the first symptoms exhibited by infected patients to minimize virus spread and give sufficient time to infected patients to mount a protective immune response.

#### ACKNOWLEDGMENTS

We thank Peter Mottram for assistance with the fluorescence microscopy. This study was supported by the Division of Biotechnology and Molecular Medicine (BioMMED) through the Governor's Biotechnology Initiative, Louisiana Board of Regents grant to KGK and personnel of the core facilities of BioMMED supported by the Center

grants NIH: NIGMS P20 GM103424 (Louisiana Biomedical Research Network) and NIH: NIGMS P20GM130555 (Center for Lung Biology) and the School of Veterinary Medicine, Louisiana State University.

#### ORCID

Konstantin G. Kousoulas  <http://orcid.org/0000-0001-7077-9003>

#### REFERENCES

1. Perlman S. Another decade, another coronavirus. *N Engl J Med*. 2020; 382(8):760-762.
2. Wu F, Zhao S, Yu B, et al. A new coronavirus associated with human respiratory disease in China. *Nature*. 2020;579(7798): 265-269.
3. Zhu N, Zhang D, Wang W, et al. A novel coronavirus from patients with pneumonia in China, 2019. *N Engl J Med*. 2020; 382(8):727-733.
4. Demmler GJ, Ligon BL. Severe acute respiratory syndrome (SARS): a review of the history, epidemiology, prevention, and concerns for the future. *Semin Pediatr Infect Dis*. 2003;14(3):240-244.
5. Vijayanand P, Wilkins E, Woodhead M. Severe acute respiratory syndrome (SARS): a review. *Clin Med*. 2004;4(2):152-160.
6. Al Mutair A, Ambani Z. Narrative review of Middle East respiratory syndrome coronavirus (MERS-CoV) infection: updates and implications for practice. *J Int Med Res*. 2020;48(1):300060519858030.
7. Badawi A, Ryoo SG. Prevalence of comorbidities in the Middle East respiratory syndrome coronavirus (MERS-CoV): a systematic review and meta-analysis. *Int J Infect Dis*. 2016;49:129-133.
8. Ramadan N, Shaib H. Middle East respiratory syndrome coronavirus (MERS-CoV): A review. *Germes*. 2019;9(1):35-42.
9. Song Z, Xu Y, Bao L, et al. From SARS to MERS, thrusting coronaviruses into the spotlight. *Viruses*. 2019;11(1):E59.
10. Du L, Zhao G, Chan CCS, et al. Recombinant receptor-binding domain of SARS-CoV spike protein expressed in mammalian, insect and E. coli cells elicits potent neutralizing antibody and protective immunity. *Virology*. 2009;393(1):144-150.
11. Bosch BJ, Martina BEE, Van Der Zee R, et al. Severe acute respiratory syndrome coronavirus (SARS-CoV) infection inhibition using spike protein heptad repeat-derived peptides. *Proc Natl Acad Sci USA*. 2004; 101(22):8455-8460.
12. Hoffmann M, Kleine-Weber H, Schroeder S, et al. SARS-CoV-2 Cell Entry Depends on ACE2 and TMPRSS2 and Is Blocked by a Clinically Proven Protease Inhibitor. *Cell*. 2010;181:271-280.e8.
13. Matsuyama S, Nagata N, Shirato K, Kawase M, Takeda M, Taguchi F. Efficient activation of the severe acute respiratory syndrome coronavirus spike protein by the transmembrane protease TMPRSS2. *J Virol*. 2010; 84(24):12658-12664.
14. Shulla A, Heald-Sargent T, Subramanya G, Zhao J, Perlman S, Gallagher T. A transmembrane serine protease is linked to the severe acute respiratory syndrome coronavirus receptor and activates virus entry. *J Virol*. 2011;85(2):873-882.
15. Bosch BJ, van der Zee R, deHaan CAM, Rottier PJM. The coronavirus spike protein is a class I virus fusion protein: structural and functional characterization of the fusion core complex. *J Virol*. 2003; 77(16):8801-8811.
16. Hofmann H, Geier M, Marzi A, et al. Susceptibility to SARS coronavirus S protein-driven infection correlates with expression of angiotensin converting enzyme 2 and infection can be blocked by soluble receptor. *Biochem Biophys Res Commun*. 2004;319(4): 1216-1221.
17. Simmons G, Gosalia DN, Rennekamp AJ, Reeves JD, Diamond SL, Bates P. Inhibitors of cathepsin L prevent severe acute respiratory syndrome coronavirus entry. *Proc Natl Acad Sci USA*. 2005;102(33): 11876-11881.



18. Triplet B, Howard MW, Jobling M, Holmes RK, Holmes KV, Hodges RS. Structural characterization of the SARS-coronavirus spike S fusion protein core. *J Biol Chem*. 2004;279(20):20836-20849.
19. Wong SK, Li W, Moore MJ, Choe H, Farzan M. A 193-amino acid fragment of the SARS coronavirus S protein efficiently binds angiotensin-converting enzyme 2. *J Biol Chem*. 2003;279(5):3197-3201.
20. Yang Z-Y, Huang Y, Ganesh L, et al. pH-dependent entry of severe acute respiratory syndrome coronavirus is mediated by the spike glycoprotein and enhanced by dendritic cell transfer through DC-SIGN. *J Virol*. 2004;78(11):5642-5650.
21. Dimitrov DS. The secret life of ACE2 as a receptor for the SARS virus. *Cell*. 2003;115(6):652-653.
22. Xia S, Zhu Y, Liu M, et al. Fusion mechanism of 2019-nCoV and fusion inhibitors targeting HR1 domain in spike protein. *Cell Mol Immunol*. <http://doi.org/10.1038/s41423-020-0374-2>
23. Wrapp D, Wang N, Corbett KS, et al. Cryo-EM structure of the 2019-nCoV spike in the prefusion conformation. *Science*. 2020;367(6483):1260-1263.
24. Pai VB, Nahata MC. Nelfinavir mesylate: a protease inhibitor. *Ann Pharmacother*. 1999;33(3):325-339.
25. Tebas P, Powderly WG. Nelfinavir mesylate. *Expert Opin Pharmacother*. 2000;1(7):1429-1440.
26. Yamamoto N, Yang R, Yoshinaka Y, et al. HIV protease inhibitor nelfinavir inhibits replication of SARS-associated coronavirus. *Biochem Biophys Res Commun*. 2004;318(3):719-725.
27. Gupta AK, Li B, Cerniglia GJ, Ahmed MS, Hahn SM, Maity A. The HIV protease inhibitor nelfinavir downregulates Akt phosphorylation by inhibiting proteasomal activity and inducing the unfolded protein response. *Neoplasia*. 2007;9(4):271-278.
28. Pajonk F, Himmelsbach J, Riess K, Sommer A, McBride WH. The human immunodeficiency virus (HIV)-1 protease inhibitor saquinavir inhibits proteasome function and causes apoptosis and radiosensitization in non-HIV-associated human cancer cells. *Cancer Res*. 2002;62(18):5230-5235.
29. Yang Y, Ikezoe T, Takeuchi T, et al. HIV-1 protease inhibitor induces growth arrest and apoptosis of human prostate cancer LNCaP cells in vitro and in vivo in conjunction with blockade of androgen receptor STAT3 and AKT signaling. *Cancer Sci*. 2005;96(7):425-433.
30. Brüning A, Burger P, Vogel M, et al. Nelfinavir induces the unfolded protein response in ovarian cancer cells, resulting in ER vacuolization, cell cycle retardation and apoptosis. *Cancer Biol Ther*. 2009;8(3):226-232.
31. Guan M, Su L, Yuan YC, Li H, Chow WA. Nelfinavir and nelfinavir analogs block site-2 protease cleavage to inhibit castration-resistant prostate cancer. *Sci Rep*. 2015;5:9698.
32. Pyrko P, Kardosh A, Wang W, Xiong W, Schonthal AH, Chen TC. HIV-1 protease inhibitors nelfinavir and atazanavir induce malignant glioma death by triggering endoplasmic reticulum stress. *Cancer Res*. 2007;67(22):10920-10928.
33. Petit CM, Chouljenko VN, Iyer A, et al. Palmitoylation of the cysteine-rich endodomain of the SARS-coronavirus spike glycoprotein is important for spike-mediated cell fusion. *Virology*. 2007;360(2):264-274.
34. Petit CM, Melancon JM, Chouljenko VN, et al. Genetic analysis of the SARS-coronavirus spike glycoprotein functional domains involved in cell-surface expression and cell-to-cell fusion. *Virology*. 2005;341(2):215-230.
35. Morris GM, Huey R, Lindstrom W, et al. AutoDock4 and AutoDockTools4: automated docking with selective receptor flexibility. *J Comput Chem*. 2009;30(16):2785-2791.
36. Kožišek M, Bray J, Řezáčová P, et al. Molecular analysis of the HIV-1 resistance development: enzymatic activities, crystal structures, and thermodynamics of nelfinavir-resistant HIV protease mutants. *J Mol Biol*. 2007;374(4):1005-1016.
37. Xia S, Liu M, Wang C, et al. Inhibition of SARS-CoV-2 (previously 2019-nCoV) infection by a highly potent pan-coronavirus fusion inhibitor targeting its spike protein that harbors a high capacity to mediate membrane fusion. *Cell Res*. 2020;30(4):343-355.
38. Podbilewicz B. Virus and cell fusion mechanisms. *Annu Rev Cell Dev Biol*. 2014;30:111-139.
39. Mothes W, Sherer NM, Jin J, Zhong P. Virus cell-to-cell transmission. *J Virol*. 2010;84(17):8360-8368.
40. Bardsley-Elliott A, Plosker GL. Nelfinavir: an update on its use in HIV infection. *Drugs*. 2000;59(3):581-620.
41. Gills JJ, LoPiccolo J, Dennis PA. Nelfinavir, a new anti-cancer drug with pleiotropic effects and many paths to autophagy. *Autophagy*. 2008;4(1):107-109.
42. Gills JJ, LoPiccolo J, Tsurutani J, et al. Nelfinavir, a lead HIV protease inhibitor, is a broad-spectrum, anticancer agent that induces endoplasmic reticulum stress, autophagy, and apoptosis in vitro and in vivo. *Clin Cancer Res*. 2007;13(17):5183-5194.
43. Harrison C. Coronavirus puts drug repurposing on the fast track. *Nat Biotechnol*. 2020;38(4):379-381.

## SUPPORTING INFORMATION

Additional supporting information may be found online in the Supporting Information section.

**How to cite this article:** Musarrat F, Chouljenko V, Dahal A, et al. The anti-HIV drug nelfinavir mesylate (Viracept) is a potent inhibitor of cell fusion caused by the SARSCoV-2 spike (S) glycoprotein warranting further evaluation as an antiviral against COVID-19 infections. *J Med Virol*. 2020;92:2087-2095. <https://doi.org/10.1002/jmv.25985>